A development of superconducting differential double contour interferometer

Vladimir L. Gurtovoi,[†,‡] Vladimir N. Antonov,[*,¶,‡] Alexey V. Nikulov,[†] Rais S. Shaikhaidarov,[¶,‡] and Vyacheslav A. Tulin[†]

[†]*Institute of Microelectronics Technology and High Purity Materials, Russian Academy of Sciences, 142432 Chernogolovka, Moscow District, Russia*

[‡]*Moscow Institute of Physics and Technology, 29 Institutskiy per., 141700 Dolgoprudny, Moscow District, Russia*

[¶]*Physics Department, Royal Holloway University of London, Egham, Surrey TW20 0EX, UK*

E-mail: v.antonov@rhul.ac.uk

Phone: +44 (0)1784443462. Fax: +44 (0)1784472794

Abstract

We study operation of a new device, the superconducting differential double contour interferometer (DDCI), in application for the ultra sensitive detection of magnetic flux and for digital read out of the state of the superconducting flux qubit. DDCI consists of two superconducting contours weakly coupled by Josephson Junctions. In such a device a change of the critical current, caused by an external magnetic flux or a nearby electric current, happens in a step-like manner when the angular momentum quantum number changes by one in one of the two contours. With a choice of parameters, the DDCI may outperform traditional Superconducting Quantum Interference Devices.

Keywords: Josephson junction, magnetometer, SQUID, superconductivity

It has been over 50 years since the first measurements of Superconducting Quantum Interference Device (SQUID), which is one of the most sensitive detectors of magnetic field. [1,2] The traditional *dc* SQUID consists of two Josephson junctions mounted in a superconducting loop. The critical current of the SQUID oscillates as $I_c = 2I_{cj}|\cos \pi\Phi_e/\Phi_0|$ for an external magnetic flux $\Phi_e = BS$ threading the loop of area S, where $\Phi_0 = h/2e$ and I_{cj} is the critical current of the individual Josephson junctions. When the *dc* SQUID is biased by a constant current I_b close to $2I_{cj}$, a periodic voltage V is developed across the *dc* SQUID when the magnetic field is varied. The effect is used in traditional *dc* SQUIDs for detection of a magnetic field $B = \Phi_e/S$. The sensitivity of the *dc* SQUID is determined by the gradient $(\partial V/\partial\Phi_e)_I$. The amplitude of the voltage oscillations δV does not exceed the value $R_d I_c < \Delta/e$, where R_d is the dynamical resistance of the Josephson junctions, Δ is the energy gap of the superconductor. [3] The mean value of $(\partial V/\partial\Phi_e)_I$ is close to $2\Delta/e\Phi_0$. For example in a *dc* SQUID made of Al, one would expect the gradient $\approx 300\ \mu V/\Phi_0$. A typical experimental value is however substantially smaller, only $\approx 2\ \mu V/\Phi_0$. In this work we explore an alternative device, a differential double contour interferometer (DDCI). It has a sensitivity to magnetic field in more than three orders of magnitude higher compared to the traditional *dc* SQUID, $\approx 13\ mV/\Phi_0$, because of a strong discreteness of the energy spectrum of the continuous superconducting loops. The DDCI has two of such loops weakly coupled by the two Josephson junctions as shown in Fig. 1. In magnetic filed there is a persistent current in each of the individual loop: [4–6]

$$I_p = \frac{n\Phi_0 - \Phi}{L_k} \tag{1}$$

In this equation n is the quantum number, $L_k = ml/sq^2n_s$ is the kinetic inductance of the loop of side l, s is the cross section of superconducting wires and n_s is the density of the Cooper pairs. The persistent current changes in a step-like manner when the quantum number n is changed. Similar to the *dc* SQUID, the voltage is developed across the DDCI when the bias current exceeds the critical value. It is the coupling of two loops by the Josephson junctions which makes the DDCI a unique magnetometer: the output signal in

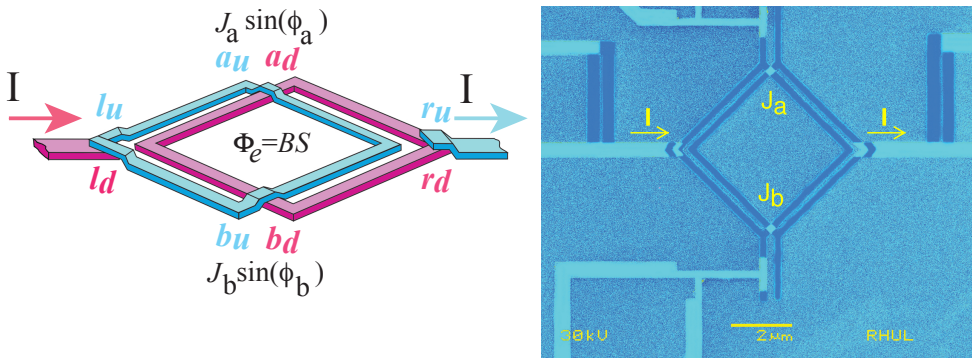

Figure 1: Design of the DDCI (left) and false colour SEM image of the experimental sample (right). In the design, two aluminium superconducting loops are weakly coupled by the Josephson junctions J_a and J_b. A bias current I from the left contact l_u of the upper loop flows through J_a and J_b to the lower loop and then to right contact r_d, whereas the persistent currents $I_p \gg I$ circulate clockwise and anticlockwise in the the upper and lower loops when the magnetic flux inside the loops, $\Phi = BS + LI_p$, is not an integer of the flux quantum, $\Phi \neq n\Phi_0$. The two loops are shifted with respect to each other so that additional loops and Josephson junctions at l_d and r_u are formed.

such a system appears as the digital step of voltage V every time the quantum number n changes in one of the loops, see Fig. 2.[7] The derivative $(\partial V/\partial \Phi_e)_I$ at the switches can be as large as 13 mV/Φ_0. Thus the DDCI behaves as a magnetometer with an extremely high sensitivity largely exceeding that of the traditional *dc* SQUID.

The superconducting current between points l_u and r_d equals to the sum of currents through the Josephson junctions J_a and J_b, see Fig.1:

$$I_s = I_a \sin \varphi_a + I_b \sin \varphi_b \tag{2}$$

Here I_a and I_b are the critical currents of the Josephson junctions, φ_a and φ_b are the phase differences between the "up", a_u and b_u, and "down", a_d and b_d, boundaries of the Josephson junctions. The relation:

$$\oint_l dl \bigtriangledown \varphi = 2\pi n \tag{3}$$

must be valid for the both contours, $l_u - a_u - r_u - b_u - l_u$ and $l_d - a_d - r_d - b_d - l_d$, in order to satisfy the requirement that the complex wave function is single-valued at any point on the

circumference l of each contour, $\Psi = |\Psi|e^{i\varphi} = |\Psi|e^{i(\varphi+n2\pi)}$. The relation (3) should be also valid for the contours $l_u - a_u - a_d - r_d - b_d - b_u - l_u$ when the current through the Josephson junctions does not exceed the critical current I_a and I_b. Then, the superconducting current between l_u and r_d is equal to:

$$I_s = I_a \sin\varphi_a + I_b \sin(\varphi_a + \pi(n_u + n_d)) \tag{4}$$

, where the quantum numbers n_d and n_u are defined as $\varphi_{au} - \varphi_{bu} = \pi n_u$ and $\varphi_{bd} - \varphi_{ad} = \pi n_d$. Here we neglect an asymmetry caused by the shift of two loops. The latter is included in the calculations given in the Section 3 of Supplement. Thus I_s depends only on parity of the quantum number sum, and it does not explicitly depend on the magnetic flux. This makes the system to be an ideal detector of the quantum states. The maximum value of the superconducting current (4) can have only two values (if one assumes $I_a = I_b = I_{cj}$): $I_s = 2I_{c,j}$, when the sum $n_u + n_d$ is even, and $I_s = 0$ when the sum is odd. Thus the critical current would be 100% modulated, and the voltage across the DDCI should jump when the quantum number n_u, or n_d, changes.

The experimental structure is fabricated using the shadow evaporation technique with aluminium metal, see the right panel of Fig.1. The films of the loops have thicknesses of 30 nm and 35 nm respectively. Aluminium is oxidised after the first evaporation in order to form Josephson junctions between the loops. The technique allows to make two independent superconducting square contours slightly shifted relative to each other and weakly connected by two Josephson junctions, J_a and J_b. There are two extra Josephson junctions at l_u and r_d. We intentionally made them large, so that the critical current of these Josephson junctions is higher than $I_a + I_b$ and the operation of DDCI was mainly determined by the latter. The DDCI structures with the loops of different sizes, $a = 4$ μm and 20 μm, were investigated. The typical width of the wires forming the loop is $w \approx 0.4$ μm so that the cross section of the wires, $\approx 10^{-14}$ m^2, is comparable to the London penetration depth

$\lambda_L^2(T) = \lambda_L^2(0)(1 - T/T_c)^{-1} \approx 8 \times 10^{-14}\ m^2$ at $T = 0.8T_c$ (for the aluminium $\lambda_L(0) \approx 50\ nm$ and the critical temperature $T_c \approx 1.3\ K$).

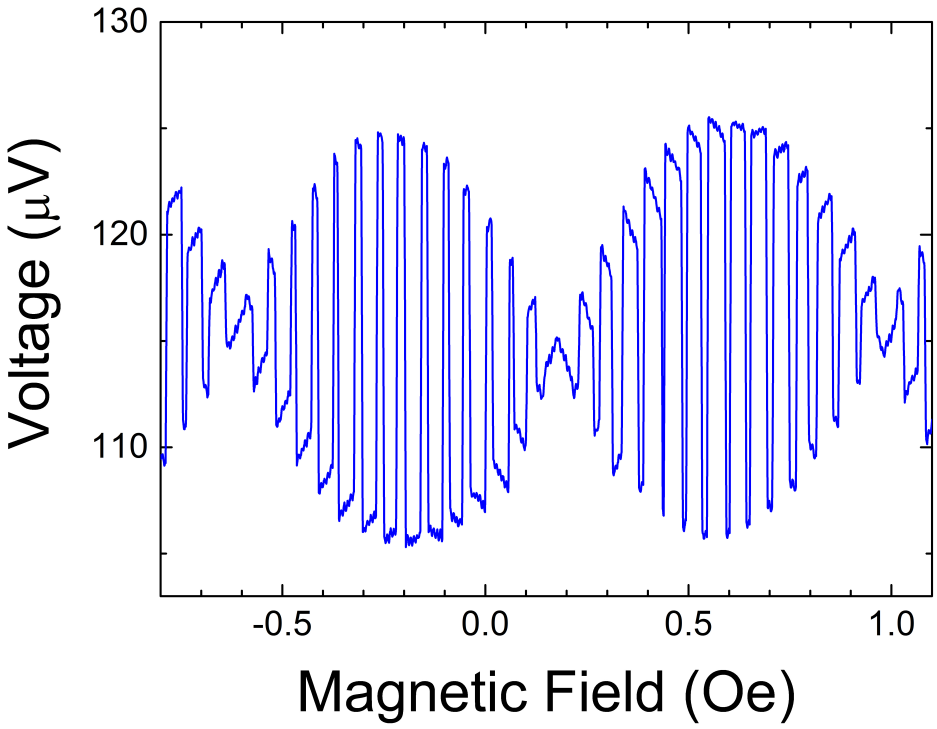

Figure 2: Voltage oscillations in DDCI with the period $B_0 \approx 0.053\ Oe$ (side of the loops $a \approx 20\ \mu m$). The transitions happen when the angular momentum quantum number, n_u or n_d, changes. The amplitude of the oscillations is modulated with the period $B_m \approx 0.8\ Oe$ corresponding to the flux through the area of two shifted loops. The DDCI is biased by $I \approx 20\ nA$ and it is kept at $T \approx 1.1\ K$.

In the experiments we indeed observe digital type oscillations of voltage, Fig. 2. The voltage jumps upwards when the sum $n_u + n_d$ becomes odd, and returns to the low value when it becomes even again. The voltage oscillates with the period corresponding to the flux quantum Φ_0 penetrating the loop. We have observed a thousand periods when sweeping the magnetic field between -30 Oe and 30 Oe.

The digital oscillations are modulated with a larger period $B_m \approx 0.8\ Oe$, which is related to the shift of two loops in the DDCI relative to each other in such a way that an additional magnetic flux penetrates through the area $S \approx 25\ \mu m^2$ inside the contour $l_u - a_u - a_d - l_d - b_d - b_u - l_u$. We refer to this contour as the shifted loop. An additional phase term

$2\pi\frac{a_{di}aB}{\Phi_0}$ appears in (4), which accounts for the modulation of switches, where $a_{di} = a_{sh}\sqrt{2}$ and $a_{sh} \approx 0.6\ \mu m$ is the shift of the upper loop relative to the bottom one. The modulation has a smooth shape because of design of the shifted loop: it is broken by the weak links, the Josephson junctions at a and b, like in the *dc* SQUID. As a result the voltage developed at the Josephson junctions has a sine shape natural for the *dc* SQUID. The shifted loop is also responsible for the asymmetry of duty cycle of digital oscillations seen in Fig. 2. The asymmetry is determined by the direction of persistent current in this loop. The phase of asymmetry of the duty cycle changes by π at the nodes of modulation, $(n_{sl} + 1/2)\ \Phi_0$, when the persistent current changes direction, n_{sl} is the number of the magnetic fluxes penetrating the shifted loop.

The current-voltage characteristics at the magnetic fields corresponding to two neighbouring values of $(n_1{+}n_2)$ are shown in Fig. 3. There are three steps at the $I - V$ curve caused by the exceeding the critical currents of the Josephson junctions at (J_a, J_b), l_u, and r_d. The critical current of the DDCI periodically changes with $(n_u{+}n_d)$. Periodic voltage jumps, seen in Fig. 2, are the difference between the the two $I - V$ curves. The amplitude of the voltage jumps has a non-linear bias current dependence.

In order to change n_u or n_d, the persistent current in one of the loops should exceed the critical value.[5,6,8] Literally this means that the pair velocity in the loop $|v_n| = (2\pi\hbar/ml)|n - \Phi/\Phi_0|$ reaches the de-pairing value $v_c = \hbar/m\sqrt{3}\xi(T)$ [9]. At low enough temperatures this happens for $|\Phi/\Phi_0| > 1$, see Fig. 4. In experiments by Vodolazov et al.[5] one would expect that $|\Phi/\Phi_0| \approx 4$. However the change of n was observed at a lower value, which was ascribed to the artificial defect in the loop. Because of high sensitivity of the DDCI even a tiny magnetic noise in measurement system may trigger the change in the quantum numbers close to the points of de-paring velocity. Otherwise the fluxes enter the loop exactly when the Cooper pair velocity is equal to the de-pairing velocity, v_c, which is highly stable. There is another factor, which may affect the periodicity: sometimes a simultaneous tunnelling of two fluxes happens, see the blue trajectories in Fig. 4. The probability of multi-flux

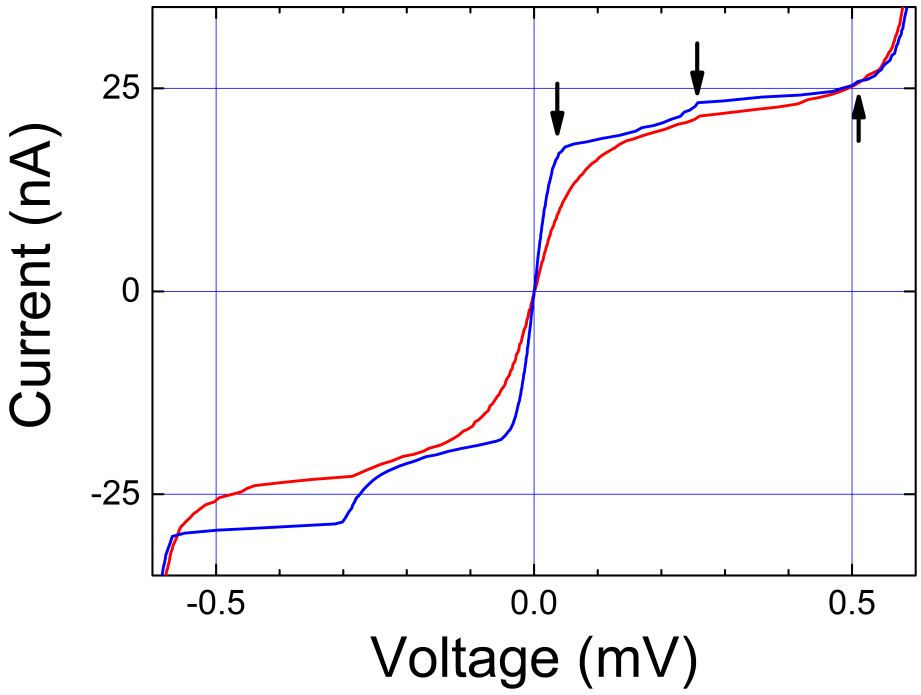

Figure 3: Two current-voltage characteristics of the DDCI when $n_u + n_d$ different by 1. There are three current steps in the curves, indicated by the arrows, which appear due to three Josephson Junctions in series: at l_u, (J_a, J_b) and at r_d. The data are taken at $T = 0.6$K

.

tunnelling events increases with the increase of v_c. One can locally decrease the threshold of the critical velocity, v_c, by using a DDCI design shown at the right panel of Fig. 4. The external current is injected to the loop segment so that v_c is effectively reduced in the loop segment for a short time. This segment can even be switched to the normal state, so that the fluxes would tunnel to the loop and n_u would change.

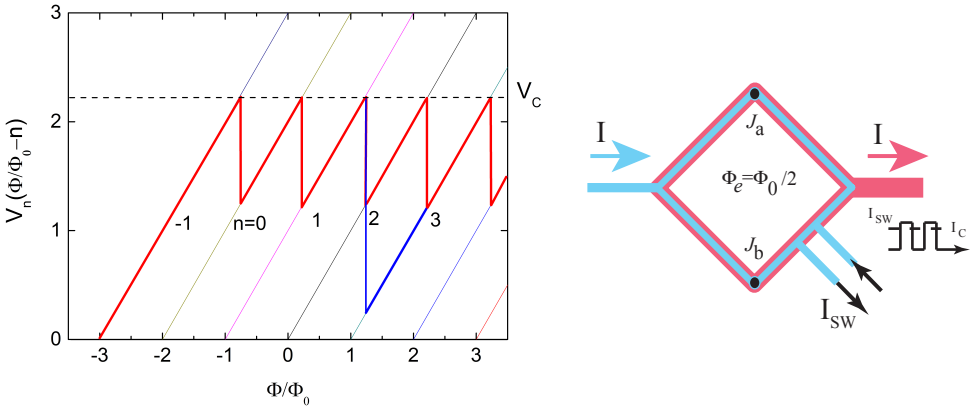

Figure 4: Left: The Cooper pair velocity and tunnelling of fluxes to the loop when external magnetic filed is varied. The tunnelling takes place when Cooper pair velocity is at v_c. There are events shown by blue trajectory when more than one flux tunnels to the loop at once. Right: Design of DDCI magnetometer where the segment of the upper loop can be switched to the normal state by short pulse of an external current I_{sw} in order to change the angular momentum quantum number n.

The DDCI is more sensitive to the change of the magnetic field compared to the conventional SQUID, because of strong discreteness of the energy spectrum of the continuous superconducting loop. The total energy of the persistent current in a loop with small cross section $s \ll \lambda_L^2(T)$ is determined mainly by the kinetic energy:

$$E_n = \frac{L_k I_p^2}{2} = \frac{\Phi_0^2}{2L_k}(n - \frac{\Phi}{\Phi_0})^2 \tag{5}$$

According to this equation, the energy difference between the adjacent permitted states n and $n+1$ is $\Phi_0^2/2L_k = I_{p,A}\Phi_0$, where $I_{p,A}$ is the persistent current at $|n - \Phi/\Phi_0| = 1/2$.[9] For a typical value of the the persistent current $I_{p,A} = 10\mu A$ the energy difference between the states corresponds to the temperature $I_{p,A}\Phi_0/k_B \approx 1500\ K$. It exceeds strongly the

temperature of the experiment $T \approx 1\ K$. As a result the state having the smallest kinetic energy predominates with a probability $P \propto \exp(-E_n/k_BT)$. This effect was confirmed in a number of experiments.[10–14] The quantum number n thus corresponds to the minimum of the kinetic energy when the last loop segments turn to the superconducting state.[15] Close to $\Phi = (n + 0.5)\Phi_0$ the two states n and $n + 1$ have a comparable probabilities. At $\Phi = (n + 0.5)\Phi_0 + \delta\Phi$ (where $\delta\Phi \ll \Phi_0$) the probability of the n state equals to:

$$P(n) \approx \frac{1}{1 + \exp(2\epsilon\frac{\delta\Phi}{\Phi_0})} \tag{6}$$

where $\epsilon = I_{p,A}\Phi_0/k_BT \gg 1$. The probability $P(n)$ changes from ≈ 1 to ≈ 0 in a narrow region of the magnetic flux, where $\delta\Phi$ varied from $-\Phi_0/2\epsilon$ to $\Phi_0/2\epsilon$. Correspondingly $P(n + 1) = 1 - P(n)$ changes reversely. A similar effect has been experimentally seen in the flux qubit with three Josephson junctions in the superconducting loop.[16] The average value of the voltage across the DDCI changes from $< V_{min} >$ to $< V_{max} >$ in this narrow region of magnetic filed. This leads to high sensitivity of the DDCI to magnetic field: $(\partial < V > /\partial\Phi_e)_I \approx 13\ mV/\Phi_0$ for the largest voltage jump observed in the experiment, $\approx 20\ \mu V$, and $\epsilon = I_{p,A}\Phi_0/k_BT \approx 1500$. The accuracy of the magnetometer improves with the increase of area S. This is in contrast to the dc SQUID, where S cannot be too large because of the strong screening in the loop with a high magnetic inductance, $L\Phi_I = LI_{c,j} > \Phi_0/2$ and $\beta = 2LI_{c,j}/\Phi_0 > 1$.[2] Because of this, a flux transformer is used in the dc SQUID for the measurement of tiny magnetic fields. In the DDCI the magnetic flux induced by the persistent current does not depend on area S since $\Phi_I = LI_p = (L/L_k)(n\Phi_0 - \Phi) \approx (s/\lambda_L^2(T))(n\Phi_0 - \Phi)$, where L is the magnetic inductance.[4] When the cross section of the loop is not small $s \geq \lambda_L^2(T)$, the total energy becomes a sum of the kinetic and magnetic energies $E_t = E_k + E_m = I_{p,A}\Phi_0(1 + L/L_k)(n - \Phi/\Phi_0)^2$. The state n with the minimal $|n - \Phi/\Phi_0|$ value has the predominant probability both at $s \ll \lambda_L^2(T)$ and at $s \geq \lambda_L^2(T)$. However, the cross section s should not be too large, since the magnetic

flux inside the loop is $\Phi = BS + LI_p$ at $I_p \neq 0$. Despite few advantages of DDCI, which we have discussed above, one needs to modify the design in order to move from the conceptual device, studied in this work, to the practical magnetometer/quantum state detector. For a purpose of magnetometer it may be re-design in a way enabling to turn a small segment of the loop for a while to the normal state, see left part of Fig.4.

In summary we demonstrate the differential double contour interferometer which can potentially outperform a conventional dc SQUID in sensitivity to small magnetic flux. The DDCI demonstrates sensitivity better than $13mV/\Phi_0$, which exceeds that of dc SQUID by more than one order of magnitude. The effect is due to the strong discreteness of the energy spectrum of the continuous superconducting loop. The advantage of DDCI lies also in circuitry, as one does not need to couple the device to a flux transformer for the measurement of small magnetic fluxes.

Acknowledgement

This work has been supported by the Russian Science Foundation, Grant No. 16-12-00070. Part of nanofabrication was done at MIPT Shared Facilities Centre supported by Grant No. RFMEFI59417X0014 of the Ministry of Education and Science of the Russian Federation.

Supporting Information. A detailed theoretical analysis of the differential double contour interferometer (DDCI) and experimental data of operation of the DDCI in a wider range of magnetic field.

References

(1) Jaklevic, R. C.; Lambe, J.; Silver, A. H.; Mercereau, J. E. *Phys. Rev. Lett.* **1964**, *12*, 159.

(2) Schwartz, B., Foner, S., Eds. *Physics and Applications of the Josephson Effect*; Plenum Press: New York, 1977.

(3) Barone, A.; Paterno, G. *Superconductor Applications: SQUIDs and Machines*; Wiley-Interscience: New York, 1982.

(4) Nikulov, A. *Quantum Studies: Mathematics and Foundations* **2016**, *3*, 41.

(5) Vodolazov, D.; Peeters, F.; Dubonos, S.; Geim, A. *Phys. Rev. B* **2003**, *67*, 054506.

(6) Bluhm, H.; Koshnick, N. C.; Huber, M. E.; Moler, K. A. *e-print arXiv: 0709.1175* **2007**,

(7) Nikulov, A. *Proceedings of 18th International Symposium NANOSTRUCTURES: Physics and Technology, St Petersburg: Ioffe Institute* **2010**, 367.

(8) Petkovich, I.; Lollo, A.; Glazman, L.; Harris, J. *Nat.Comm.* **2016**, *7*, 13551.

(9) Tinkham, M. *Introduction to Superconductivity*; McGraw-Hill Book Company: New York, 1975.

(10) Gurtovoi, V.; Dubonos, S.; Nikulov, A.; Osipov, N.; Tulin, V. *JETP* **2007**, *105*, 1157.

(11) Gurtovoi, V.; Exarchos, M.; Antonov, V.; Nikulov, A.; Tulin, V. *App. Phys. Lett.* **2016**, *109*, 032602.

(12) Gurtovoi, V.; Dubonos, S.; Karpin, S.; Nikulov, A.; Tulin, V. *JETP* **2007**, *105*, 262.

(13) Koshnick, N.; Bluhm, H.; Huber, M. E.; Moler, K. *Science* **2007**, *318*, 1440.

(14) Burlakov, A.; Gurtovoi, V.; Ilin, A.; Nikulov, A.; Tulin, V. *Phys. Lett. A* **2012**, *376*, 2325.

(15) Gurtovoi, V.; Nikulov, A. *Phys. Rev. B* **2014**, *90*, 056501.

(16) Tanaka, H.; Saito, S.; Nakano, H.; Semba, K.; Ueda, M.; Takayanagi, H. *arXiv:cond-mat/0407299* **2004**,

Graphical TOC Entry